ACS Medicinal Chemistry Letters

LETTER

pubs.acs.org/acsmedchemlett

3D Pharmacophore Model-Assisted Discovery of Novel CDC7 Inhibitors

Mika Lindvall,* Christopher McBride, Maureen McKenna, Thomas G. Gesner, Asha Yabannavar, Kent Wong, Song Lin, Annette Walter, and Cynthia M. Shafer*

Global Discovery Chemistry/Oncology & Exploratory Chemistry, Novartis Institutes for Biomedical Research, 4560 Horton Street, Emeryville, California 94608, United States

Supporting Information

ABSTRACT: A ligand-based 3D pharmacophore model for serine/threonine kinase CDC7 inhibition was created and successfully applied in the discovery of novel 2-(heteroaryl)-6,7-dihydrothieno[3,2-c]pyridin-4(5*H*)-ones. The pharmacophore model provided a hypothesis for lead generation missed by docking to a homology model. Medicinal chemistry exploration of the series revealed clear structure−activity relationships consistent with the pharmacophore model and pointed to further optimization opportunities.

KEYWORDS: CDC7, kinase, pharmacophore model, homology model, lead generation, structure−activity relationship

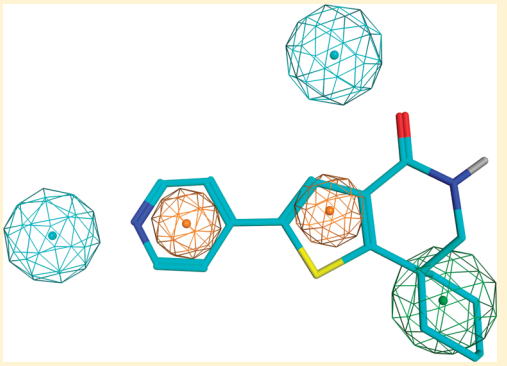

The serine/threonine kinase CDC7 plays an essential role in the initiation of DNA replication in eukaryotic cells.[1] After assembly of the prereplication complex to the replication origin, the CDC7 kinase phosphorylates MCM (minichromosome maintenance) proteins and allows for recruitment of CDC45 and DNA polymerase, thereby initiating DNA replication.[2] CDC7 requires association with one of its cofactors, ASK (also known as DBF4) or ASKL1 (also known as Drf1), for kinase activation.[3−6]

Recently, CDC7 has emerged as an attractive target for cancer therapy.[7−9] Depletion of CDC7 using siRNA oligonucleotides results in induction of apoptosis in cancer cell lines, while normal dermal fibroblast cells are spared.[10] Furthermore, CDC7-mediated phosphorylation sites on MCM2, MCM4, and MCM6 in tumor cells have been identified, but the functional relevance of those sites remains to be determined.[11−14]

Our group was pursuing additional lead generation techniques for the development of a CDC7 inhibitor.[15] In the absence of a CDC7 crystal structure, a 3D pharmacophore hypothesis was developed to guide the chemistry efforts. The model was created from two CDC7 compounds reported in the literature, **1**[16,17] and **2**[18] (Figure 1), via flexible superimposition of their 3D models,[19,20] and identification of the three-dimensional (3D) features that they shared. Several different overlays of **1** and **2** were considered,[21] with the preferred pharmacophore model (Figure 2) consisting of four shared features, two acceptor projected points F1 and F4, and two aromatic rings F2 and F3. While such features are relatively generic for kinases, an additional hydrophobic feature F5 was appended to the model based on structure−activity relationship (SAR) where the allyl group in **2** selectively increases CDC7 potency (**2** and **3**) versus CDK2 potency (Figure 2).[22] Consequently, the final five-feature pharmacophore model consisted of four common features (**C**) and one SAR-based feature (**S**). Of equal importance, the superimposition of **1** and **2** suggested that certain hydrogen-bonding features were not critical for potency as they were absent (**A**) in one of the two molecules. The pyrrole hydrogen bond donor in **1** was determined to be the least critical due to overlap with a methyl in **2**. Thus, the availability of rigid molecules with comparable shapes, informative distribution of functional groups, and access to SAR facilitated the creation of a pharmacophore model for CDC7 activity.

A homology model for CDC7 was also built, using CK2 as the template.[23,24] Although **1**−**3** could be docked to the model and the likely hinge binding groups in **1**−**3** could be readily identified,[21] the remaining portions of the molecules were poorly aligned, and the ligand overlay in Figure 2 was not identified from poses with optimal interactions to the protein. In addition, no obvious hydrophobic pocket was found around the allyl group in **2** in any of the poses. The hypothesis formed from the pharmacophore model in Figure 2 suggests where to place a hydrophobic group (F5), and such chemistry guidance was not available from docking to the homology model. Consequently, ligand-based models such as a pharmacophore model can sometimes provide clearer hypotheses than those obtained from homology models. In particular, key hypotheses may appear less likely or may be missed altogether due to challenges in docking to models with

Received: February 2, 2011
Accepted: June 15, 2011
Published: August 02, 2011

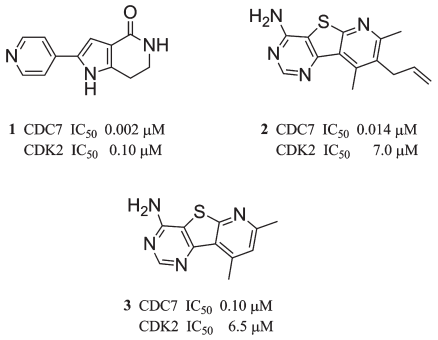

Figure 1. CDC7 inhibitors for pharmacophore model generation.

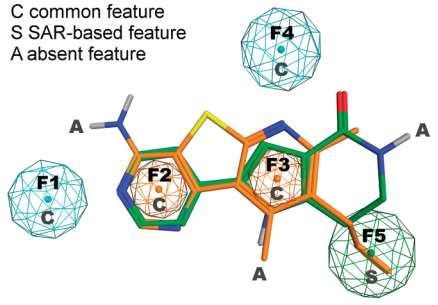

Figure 2. 3D pharmacophore model for CDC7 inhibition.

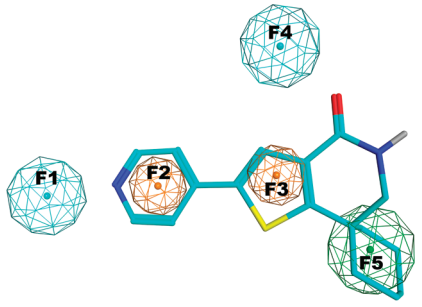

Figure 3. Compound **4** mapped onto the pharmacophore model.

low homology between the template and the protein of interest. For CDC7, the SAR-driven features and direct chemistry guidance made the pharmacophore model preferable for lead generation efforts.

The next step was to test the pharmacophore model and apply it in the design of novel CDC7 inhibitors. As sufficiently large 3D databases of internal and vendor compounds were not available at the time when this work was carried out, the typical step of pharmacophore validation by 3D database searching and hit rate analysis was not performed. Instead, 2D databases were searched with a SMARTS query, and the results were refined in 3D applying the pharmacophore model. Initially, molecules were sought that would closely match all of the core features and would explore different hydrophobes.[25] As no suitable hits were found, a new 2D query was used that could map onto features F3−F5 but had a chemical handle, allowing introduction of moieties that would map onto features F1−F2.[26] The query hits were converted to a small virtual library by transforming the chemical handle to a 4-pyridyl moiety. The virtual library was evaluated by 3D pharmacophore searching using our CDC7 pharmacophore hypothesis (Figure 2). One of the hits was **4**, derived from commercially available advanced intermediate **22** (Table 1).

Compound **4** has an excellent match to the pharmacophore model (Figure 3). It matches all five features, including the hydrophobe F5 specifically added for CDC7, and superimposition with **2** shows a very good overlap between the allyl group in **2** and the spiro-cyclohexyl group in **4**. Superimposition of **1** and **4** where thiophene sulfur and pyrrole NH overlap shows that if a donor feature from pyrrole NH was included in the pharmacophore model, **4** would not have been identified.

Compound **4** proved to be quite potent against CDC7/DBF4 in vitro (Table 1). Thus, using **22**, analogues of **4** could be prepared, allowing rapid expansion of the SAR and evaluation of the limits of the pharmacophore model.[27]

In a retrospective analysis of the CDC7 assay data, the SAR is in good agreement with the assumption that the heterocycle group maps to the hinge region. As expected of pharmacophore models, the agreement with the model and the data is not quantitative. Compound pair **4**−**5** shows the importance of the hydrogen-bonding direction, and the drop in potency is expected. Similarly, the lack of an acceptor in **8** causes an expected drop in potency. Examples **6**, **7**, **10**, and **11** are typical of kinase hinge SAR, where a key acceptor with the right hydrogen-bonding directionality is retained and an additional donor for the hinge is tolerated, with or without potency increase. The lack of potency in **9** and **12**, on the other hand, is likely to be caused by steric clashes with the hinge of CDC7. The steric clash hypothesis in **9** is consistent with the pharmacophore model, as the methyl amide donor of **9** overlaps with the acceptor projected point F1 in the pharmacophore model where a protein donor atom from the hinge of CDC7 is expected. In compound **11**, the pyrazole NH is assumed to make a hydrogen-bonding contact with a carbonyl of the hinge, so methylation of the NH yielding **12** is expected to result in a steric clash.[28] Such steric clashes can be incorporated as iterative, SAR-based refinements into the pharmacophore model via addition of excluded volumes.

Because the pharmacophore model indicated that hydrophobic groups would be favored at C6 and C7, only analogues with a spiro-cyclohexyl appended to the pyridone ring had been synthesized up to this point. Removal of the cyclohexyl group was desired to test one of the key hypotheses formed from the pharmacophore model. Compound **14**, which lacks the hydrophobic spiro-cyclohexyl group, has at least 30-fold lower potency against CDC7 than **4**, suggesting that the spiro-cyclohexyl moiety has the same potency-enhancing properties as the allyl group in **2**.

Upon determining that the spiro-cyclohexyl moiety was important for biochemical activity, the role of the pyridone nitrogen on in vitro potency was then evaluated. Compounds (**15**−**17**) were synthesized where the lactam nitrogen was replaced with a CH_2. In the cases of the pyridyl and aminopyridyl hinge binders (**15** and **16**), a loss of 4−8-fold in potency was observed as compared to **4** and **6**, while compound **17** remained equipotent to **11**.

In retrospect, it is educational to review how the advanced intermediate **22** and the resulting initial hit **4** could have been identified for CDC7 with other computational approaches.[29] While a rigorous retrospective study would require appropriate molecule databases including decoy molecules to study enrichment, recovery, and practical caveats, 2D and 3D similarity comparisons can hint at how well **22** and our novel series might

dx.doi.org/10.1021/ml200029w |ACS Med. Chem. Lett. 2011, 2, 720–723

Table 1. SAR of the Thienopyridinone Series

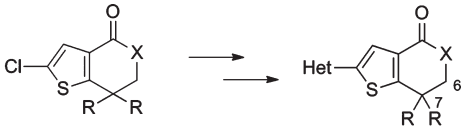

22 X = NH, R, R = -$(CH_2)_5$-

Cmpd	Het	X	R	CDC7 DBF4 IC_{50} (μM)	Cmpd	Het	X	R	CDC7 DBF4 IC_{50} (μM)
4		NH	-$(CH_2)_5$-	<0.001	**11**		NH	-$(CH_2)_5$-	0.001
5		NH	-$(CH_2)_5$-	5.1	**12**		NH	-$(CH_2)_5$-	>25
6		NH	-$(CH_2)_5$-	0.008	**13**		NH	-$(CH_2)_5$-	0.37
7	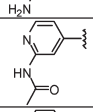	NH	-$(CH_2)_5$-	0.041	**14**		NH	H,H	0.033
8	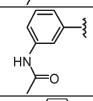	NH	-$(CH_2)_5$-	>25	**15**		CH_2	-$(CH_2)_5$-	0.009
9	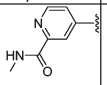	NH	-$(CH_2)_5$-	>25	**16**		CH_2	-$(CH_2)_5$-	0.033
10		NH	-$(CH_2)_5$-	0.001	**17**		CH_2	-$(CH_2)_5$-	0.001

have scored at the computational idea evaluation stage. Compounds **1** and **14** differ only by a single NH to S substitution, with **14** being 15 times less potent than **1**. The 2D Tanimoto similarity between **1** and **14**, which have the same number of heavy atoms, was surprisingly low, ranging from 0.39 to 0.51 using Daylight fingerprints or ECFPs or FCFPs from SciTegic. Consequently, traditional 2D approaches would likely have failed to highlight **22** as is or even after virtual conversion into products such as **4** and **14**, when compared to **1** or other literature examples related to **1**.[30]

In sharp contrast, field-based 3D similarity using the commercial Cresset package[31] between **1** and **14** is very high, 0.91. Moderate to high 3D similarities of 0.6−0.8 are observed between the starting points **1**−**3** and **4**. Even the intermediate **22** itself is 0.65−0.69 similar to **1**−**3** and up to 0.82 for other reported examples related to **1**.[30] Similarities to **22** are unexpectedly high, as the lack of an aromatic ring corresponding to F2 was assumed to significantly reduce similarity in a whole-molecule similarity calculation.[32] Consequently, even whole-molecule 3D similarity searching would probably have highlighted desirable intermediates such as **22**. Finally, 3D pharmacophore searching can be tuned to specifically look for relevant advanced intermediates. For example, **22** is a hit with an rmsd of 0.3 with a query derived from the pharmacophore in Figure 2 where F1 is deleted and F2 is changed to a volume feature for Suzuki chemistry compatible atoms.[33,34] In summary, 3D approaches can successfully circumvent the failure of traditional 2D fingerprint similarity in the discovery of the intermediate **22** and the corresponding initial hit **4**.

In conclusion, a ligand-based 3D pharmacophore model was developed from known CDC7 inhibitors and provided clearer chemistry guidance for lead generation than docking to a low-resolution homology model. The pharmacophore model was successfully applied in the discovery of a novel thienopyridone series made in a single step from commercially available material. Additional analogues were designed and synthesized to create a series of inhibitors with clear SAR where simple modifications yielded at least 2 orders of magnitude changes in potency. Furthermore, the SAR was consistent with the pharmacophore model and identified ways for refining the model.

■ ASSOCIATED CONTENT

Supporting Information. Experimental details for the synthesis and characterization of select compounds, procedures for the biochemical and cellular assay, and additional information on the computational methods utilized. This material is available free of charge via the Internet at http://pubs.acs.org.

■ AUTHOR INFORMATION

Corresponding Authors

*Tel: 510-923-8086. E-mail: cynthia.shafer@novartis.com (C.M.S.). Tel: 510-923-3312. E-mail: mika.lindvall@novartis.com (M.L.).

■ ACKNOWLEDGMENT

We thank Dazhi Tang for his mass spectroscopy support, and Dachuan Lei providing the A549 cells required for stability studies.

REFERENCES

(1) Jiang, W.; McDonald, D.; Hope, T. J.; Hunter, T. Mammalian Cdc7-Dbf4 protein kinase complex is essential for initiation of DNA replication. *EMBO J.* **1999**, *18* (20), 5703.

(2) Kim, J. M.; Yamada, M.; Masai, H. Functions of mammalian Cdc7 kinase in initiation/monitoring of DNA replication and development. *Mutat. Res.* **2003**, *532* (1, 2), 29.

(3) Ogino, K.; Takeda, T.; Matsui, E.; Iiyama, H.; Taniyama, C.; Arai, K.-I.; Masai, H. Bipartite binding of a kinase activator activates Cdc7-related kinase essential for S phase. *J. Biol. Chem.* **2001**, *276* (33), 31376.

(4) Sato, N.; Sato, M.; Nakayama, M.; Saitoh, R.; Arai, K.-I.; Masai, H. Cell cycle regulation of chromatin binding and nuclear localization of human Cdc7-ASK kinase complex. *Genes Cells* **2003**, *8* (5), 451.

(5) Montagnoli, A.; Bosotti, R.; Villa, F.; Rialland, M.; Brotherton, D.; Mercurio, C.; Berthelsen, J.; Santocanale, C. Drf1, a novel regulatory subunit for human Cdc7 kinase. *EMBO J.* **2002**, *21* (12), 3171.

(6) Yoshizawa-Sugata, N.; Ishii, A.; Taniyama, C.; Matsui, E.; Arai, K.-I.; Masai, H. A Second Human Dbf4/ASK-related Protein, Drf1/ASKL1, Is Required for Efficient Progression of S and M Phases. *J. Biol. Chem.* **2005**, *280* (13), 13062.

(7) Swords, R.; Mahalingam, D.; O'Dwyer, M.; Santocanale, C.; Kelly, K.; Carew, J.; Giles, F. Cdc7 kinase—A new target for drug development. *Eur. J. Cancer* **2010**, *46* (1), 33.

(8) Montagnoli, A.; Moll, J.; Colotta, F. Targeting Cell Division Cycle 7 Kinase: A New Approach for Cancer Therapy. *Clin. Cancer Res.* **2010**, *16* (18), 4503.

(9) Rodriguez-Acebes, S.; Proctor, I.; Loddo, M.; Wollenschlaeger, A.; Rashid, M.; Falzon, M.; Prevost, A. T.; Sainsbury, R.; Stoeber, K.; Williams, G. H. Targeting DNA Replication before it Starts: CDC7 as a Therapeutic Target in p53-Mutant Breast Cancers. *Am. J. Pathol.* **2010**, *177*, 2034.

(10) Montagnoli, A.; Tenca, P.; Sola, F.; Carpani, D.; Brotherton, D.; Albanese, C.; Santocanale, C. Cdc7 inhibition reveals a p53-dependent replication checkpoint that is defective in cancer cells. *Cancer Res.* **2004**, *64* (19), 7110.

(11) Montagnoli, A.; Valsasina, B.; Brotherton, D.; Troiani, S.; Rainoldi, S.; Tenca, P.; Molinari, A.; Santocanale, C. Identification of Mcm2 Phosphorylation Sites by S-phase-regulating Kinases. *J. Biol. Chem.* **2006**, *281* (15), 10281.

(12) Tsuji, T.; Ficarro, S. B.; Jiang, W. Essential role of phosphorylation of MCM2 by Cdc7/Dbf4 in the initiation of DNA replication in mammalian cells. *Mol. Biol. Cell* **2006**, *17* (10), 4459.

(13) Masai, H.; Taniyama, C.; Ogino, K.; Matsui, E.; Kakusho, N.; Matsumoto, S.; Kim, J.-M.; Ishii, A.; Tanaka, T.; Kobayashi, T.; Tamai, K.; Ohtani, K.; Arai, K.-I. Phosphorylation of MCM4 by Cdc7 Kinase Facilitates Its Interaction with Cdc45 on the Chromatin. *J. Biol. Chem.* **2006**, *281* (51), 39249.

(14) Sheu, Y.-J.; Stillman, B. Cdc7-Dbf4 phosphorylates MCM proteins via a docking site-mediated mechanism to promote S phase progression. *Mol. Cell* **2006**, *24* (1), 101.

(15) Shafer, C. M.; Lindvall, M.; Bellamacina, C.; Gesner, T. G.; Yabannavar, A.; Jia, W.; Lin, S.; Walter, A. 4-(1H-Indazol-5-yl)-6-phenylpyrimidin-2(1H)-one analogs as potent CDC7 inhibitors. *Bioorg. Med. Chem. Lett.* **2008**, *18* (16), 4482.

(16) Vanotti, E.; Amici, R.; Bargiotti, A.; Berthelsen, J.; Bosotti, R.; Ciavolella, A.; Cirla, A.; Cristiani, C.; D'Alessio, R.; Forte, B.; Isacchi, A.; Martina, K.; Menichincheri, M.; Molinari, A.; Montagnoli, A.; Orsini, P.; Pillan, A.; Roletto, F.; Scolaro, A.; Tibolla, M.; Valsasina, B.; Varasi, M.; Volpi, D.; Santocanale, C. Cdc7 kinase inhibitors: Pyrrolopyridinones as potential antitumor agents. 1. Synthesis and structure-activity relationships. *J. Med. Chem.* **2008**, *51* (3), 487.

(17) Menichincheri, M.; Bargiotti, A.; Berthelsen, J.; Bertrand, J. A.; Bossi, R.; Ciavolella, A.; Cirla, A.; Cristiani, C.; Croci, V.; D'Alessio, R.; Fasolini, M.; Fiorentini, F.; Forte, B.; Isacchi, A.; Martina, K.; Molinari, A.; Montagnoli, A.; Orsini, P.; Orzi, F.; Pesenti, E.; Pezzetta, D.; Pillan, A.; Poggesi, I.; Roletto, F.; Scolaro, A.; Tato, M.; Tibolla, M.; Valsasina, B.; Varasi, M.; Volpi, D.; Santocanale, C.; Vanotti, E. First Cdc7 Kinase Inhibitors: Pyrrolopyridinones as Potent and Orally Active Antitumor Agents. 2. Lead Discovery. *J. Med. Chem.* **2009**, *52* (2), 293.

(18) Zhao, C.; Tovar, C.; Xuefeng, Y.; Xu, Q.; Todorov, I. T.; Vassilev, L. T.; Chen, L. Synthesis and evaluation of pyrido-thieno-pyrimidines as potent and selective Cdc7 kinase inhibitors. *Bioorg. Med. Chem. Lett.* **2009**, *19*, 319.

(19) Labute, P.; Williams, C.; Feher, M.; Sourial, E.; Schmidt, J. M. Flexible Alignment of Small Molecules. *J. Med. Chem.* **2001**, *44*, 1483.

(20) As implemented in MOE 2004. Chemical Computing Group Inc., 1010 Sherbooke St. West, Suite #910, Montreal, QC, Canada, H3A 2R7.

(21) Additional details available in the Supporting Information.

(22) The solubilities of **2** and **3** are within 2-fold (1.3 and 0.65 μM, respectively) and do not account for the 7-fold potency difference. In addition, the solubilities of the **2** and **3** are, respectively, >90- and >6-fold higher than the IC_{50} values, giving good confidence in the quality of the data. Finally, the dose−response curves at high concentrations do not show signs of precipitation.

(23) Homology modeling was carried out with MOE, using CK2 coordinates as the template (PDB code 1lp4).

(24) There is 21% sequence identity between CDC7 (kinase domain without CDC7 specific insert domain) and CK2. In the active site, there is a 42% sequence identity (within 5Å from ATP of 1lp4).

(25) SMARTS query a1[C](=O)AAAa1ac(-a)a.

(26) SMARTS query a1[C](=O)AAAa1ac([Cl,Br,I])a.

(27) Synthetic details for select analogues are available in the Supporting Information.

(28) The inactivity of **12** gives further support to the proposed SAR interpretation. Additional details are available in the Supporting Information.

(29) The advanced intermediate **22** itself is inactive, CDC7 IC_{50} > 25 μM.

(30) Vanotti, E.; D'Alessio, R.; Tibolla, M.; Varasi, M.; Montagnoli, A.; Santocanale, C.; Martina, K.; Menichincheri, M. Pyridylpyrrole Derivatives Active as Kinase Inhibitors. WO2005013986, 2005.

(31) FieldAlign version 2.1.0. Default settings of 50% shape and 50% field contributing to the reported overall 3D similarity. Cresset, Broadwater Road, Welvyn Garden City AL7 3AX, United Kingdom.

(32) Tversky similarity (Leach, A. R.; Gillet, V. J. *An Introduction to Chemoinformatics*; Kluwer Academic Publishers: Dordrecht, The Netherlands, 2003) was not available in FieldAlign.

(33) Volume feature matching SMARTS [$([Cl,Br,I,B]a)].

(34) Addition of exterior volume or excluded volumes would enhance enrichment of intended intermediates in case a large number of hits were obtained.